# Atomic diffusion studied with coherent X-rays

**Michael Leitner**[*], **Bogdan Sepiol**[1], **Lorenz-Mathias Stadler**[2], **Bastian Pfau**[3] **and Gero Vogl**[1]

Knowledge of atomic diffusion is a fundamental issue in synthesis and stability of materials. Direct studies of the elementary diffusion event, i.e. how the individual atoms "jump", are scarce, as the available techniques are limited to selected systems[1]. Here we show how by monitoring the spatial and temporal variations of the scattered coherent X-ray intensity the diffusion of single atoms can be studied. This is demonstrated for the intermetallic alloy $Cu_{90}Au_{10}$. By measuring along several directions in reciprocal space we can elucidate the dynamical behaviour of single atoms as a function of their neighbourhood. This method, usually referred to as X-ray photon correlation spectroscopy (XPCS)[2-5], does not rely on specific atomic species or isotopes and can thus be applied to almost any system. Given the advent of the next-generation X-ray sources we envision XPCS to become the main method for quantitatively understanding diffusion on the atomic scale.

Diffusion in solids is conventionally studied by profiling the depth dependence of tracer atoms diffused into the sample[6]. This gives only a macroscopic quantity, the diffusion constant. The question of how diffusion happens on the atomic scale is more fundamental. For a few systems, this question has been answered by applying quasielastic neutron scattering[1,7] and Mößbauer spectroscopy, the latter with radioactive sources or synchrotron radiation[1]. These methods suffer, however, from their limitation to a narrow number of isotopes and to a rather limited range of (very fast) diffusivities, challenging their relevance for questions of, e.g., materials stability at ambient temperatures. Thus, there is doubtlessly the demand for a universal method for studying dynamics with atomic resolution and the sensitivity to slower dynamics.

In this paper we present the first successful study of atomic diffusion using the technique of XPCS, which is based on the scattering of coherent X-rays. Generally, with XPCS one measures the temporal evolution of fluctuations in the electron density as a function of the wave vector **q** of scattered radiation. In our case the sample consists of a single crystal of a binary alloy, so the electron density directly corresponds to the lattice sites' occupation state. Since in equilibrium fluctuations decay due to stochastic diffusive motion of the individual atoms, probing the decay times as a function of the crystallographic direction allows to draw conclusions on the motion of the atoms on the lattice. The relevant information corresponding to atomic scales is in the diffuse scattering regime, contrary to studies of comparatively big objects[4] or large-scale lattice defects[3,5] using small-angle scattering or measuring in and around Bragg reflections, respectively.

We studied atomic diffusion in the system $Cu_{90}Au_{10}$ at temperatures around 540 K, where the system is a substitutional solid solution, i.e. the Au atoms statistically occupy sites in the Cu face-centred cubic lattice. Throughout the Cu–Au phase diagramme a tendency favouring nearest-neighbour pairs of unlike atoms is

discernible. Ref. 8 confirms this image for our sample at an even slightly elevated temperature (573 K): the probability for occurrence of nearest-neighbour Au pairs is much lower than in a perfectly random configuration, second nearest-neighbour Au pairs are more frequent, and so on, with the deviations diminishing towards zero for large distances.

We positioned an oriented single crystal of $Cu_{90}Au_{10}$ inside a furnace in a partially coherent X-ray beam at beamline ID10A at the European Synchrotron Radiation Facility in Grenoble, France. Time series of scattered intensity were recorded with a pixel detector for a number of detector positions, i.e. different scattering vectors, and temperatures. These time series were interpreted in terms of the intensity auto-correlation function

$$g^{(2)}(\mathbf{q}, \Delta t) = \frac{\langle I(\mathbf{q}, .)I(\mathbf{q}, . + \Delta t)\rangle}{\langle I(\mathbf{q}, .)\rangle^2}. \qquad (1)$$

The intensity for a given scattering vector **q** at a given time is correlated with the intensity at the same **q** at a time $\Delta t$ later and is normalised by the square of the expectation of the intensity. As under equilibrium conditions only the time delay matters, the ensemble average in Eq. (1) can be realised via averaging over absolute time and the detector pixels.

In real space, dynamic processes are described by van Hove's pair correlation function $G(\Delta \mathbf{x}, \Delta t)$[9]. In case of a binary alloy, where the constituents occupy the sites of a discrete lattice, $G(\Delta \mathbf{x}, \Delta t)$ has a very intuitive interpretation: it is the probability for site $\Delta \mathbf{x}$ to be occupied at time $\Delta t$ by an atom of sort A under the condition that site $\mathbf{0}$ was occupied at time 0 by an atom of sort A. It turns out that $G(\Delta \mathbf{x}, \Delta t)$ and $g^{(2)}(\mathbf{q}, \Delta t)$ are related via a spatial Fourier transform (denoted by $\mathscr{F}(.)$):

$$g^{(2)}(\mathbf{q}, \Delta t) = 1 + \beta \left(\frac{\mathscr{F}(G(., \Delta t))(\mathbf{q})}{\mathscr{F}(G(., 0))(\mathbf{q})}\right)^2 \qquad (2)$$

see, e.g., Ref. 10 for a detailed derivation. Ideally, the coherence factor $\beta$ is unity, but partial coherence, thermal vibrations of atoms, inelastic background scattering, and finite detector pixel sizes lead to smaller $\beta$.

Since XPCS is the time domain counterpart of coherent Quasi-Elastic Neutron Scattering (QENS), which operates in the energy domain, concepts developed for QENS apply for XPCS as well. The quasi-elastic line-width $\Gamma(\mathbf{q})$ corresponds to decay times via $\tau(\mathbf{q}) = \Gamma(\mathbf{q})^{-1}$, and so the intensity auto-correlation function of a dilute substitutional alloy on a Bravais lattice is given by

$$g^{(2)}(\mathbf{q}, \Delta t) = 1 + \beta e^{-2\Delta t/\tau(\mathbf{q})}, \qquad (3)$$

$$\tau(\mathbf{q}) = \tau_0 \frac{1}{1 - \sum_i p_i \cos(\mathbf{s}_i \mathbf{q})}. \qquad (4)$$

[1]Fakultät für Physik, Universität Wien, Strudlhofgasse 4, 1090 Wien, Austria, [2]HASYLAB at DESY, Notkestr. 85, 22607 Hamburg, Germany, [3]Helmholtz-Zentrum Berlin für Materialien und Energie GmbH, Glienicker Str. 100, 14109 Berlin, Germany. *e-mail: michael.leitner@univie.ac.at.
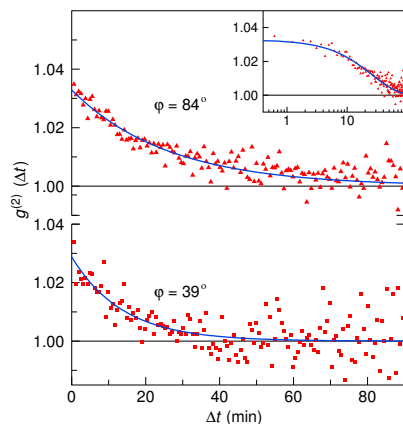
**Figure 1 | Variation of temporal intensity auto-correlations with position in reciprocal space.** Shown are measurements at fixed temperature 543 K, fixed scattering angle $2\theta = 25°$, and varying azimuthal angles $\varphi = 84°$ and $\varphi = 39°$ (for definition of angles see Fig. 3) with fitted exponential decays. Even though the modulus of the scattering vector is the same, the fitted correlation times ($52 \pm 5$ min for $\varphi = 84°$ and $28 \pm 4$ min for $\varphi = 39°$, respectively) differ by a factor of two. The inset shows the measurement with $\varphi = 84°$ plotted on a logarithmic time scale.

Here $\tau_0$ is the mean residence time between jumps of the solute atoms, $\mathbf{s}_i$ are the possible jump vectors and $p_i$ the respective probabilities[11]. For exclusively nearest-neighbour jumps, the probabilities $p_i$ are equal to the inverse of the coordination number. The interpretation of the experimental data is carried out by fitting Eq. (3) to the measured intensity auto-correlation functions Eq. (1) as shown in Fig. 1. The fitted decay time $\tau(\mathbf{q})$ is the lifetime of fluctuations corresponding to the wave vector $\mathbf{q}$ and, thus, gauges the dynamics in the sample.

Regardless of the actual mechanism of diffusion, the influence of temperature on the dynamics of the system manifests itself in the jump frequency and therefore in the decay time. We did measurements at fixed $\mathbf{q}$ in the temperature range of 528 K–555 K. As can be seen in Fig. 2, the findings can be reproduced by assuming an Arrhenius dependence between jump frequency and temperature. The fitted activation enthalpy $E_A = (2.09 \pm 0.15)$ eV is the sum of the formation enthalpy of a vacancy and the migration enthalpy, the barrier an atom has to overcome when jumping into a vacancy. It agrees with extrapolations from high-temperature tracer diffusion measurements to our temperature range[12].

Proceeding from an ideal solid solution, where the solutes do not interact, to a system with significant short-range order, new effects come into play: The neighbourhood of an atom starts to influence its jump behaviour. Following the argumentation of de Gennes[13], local atomic configurations which are energetically favoured will be more stable with respect to diffusional decay than energy-costly configurations, and they will also be more frequent. Conversely, values of $\mathbf{q}$ with high diffuse scattering intensities (short-range order's equivalent of superstructure-peaks) correspond to energetically favoured and therefore long-lived fluctuations. The QENS analogue would be the narrowing of the quasi-elastic line width at this $\mathbf{q}$, which is also known as de Gennes-narrowing[14,15].

This problem is treated quantitatively in Ref. 16 in a mean field theory of linear response. Transferring their results from the energy into the time domain, one observes that the decay of $g^{(2)}(\mathbf{q}, \Delta t)$ retains its exponential form as in the dilute, non-interacting case, compare Eq. (3). However, the decay time $\tau(\mathbf{q})$ has to be modified:

$$\tau(\mathbf{q}) = \tau_0 \frac{I_{\text{SRO}}(\mathbf{q})}{1 - \sum_i p_i \cos(\mathbf{s}_i \mathbf{q})} \qquad (5)$$
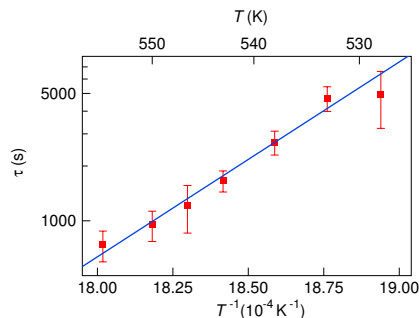


**Figure 2 | Influence of temperature on dynamics.** Error bars are standard errors of the fitted correlation times. The position of the measurement is $2\theta = 25°$ and $\varphi = 39°$. Note that the correlation time $\tau$ is inversely proportional to the jump frequency, giving a positive slope.

The quantity $\tau_0$ is the mean time between atomic exchanges. The short-range order intensity $I_{\text{SRO}}$ is measured in units relative to its average over all directions (the so-called Laue units), so with no variations in the diffuse intensity (no short-range order) Eq. (5) reduces to Eq. (4). Here is where de Gennes-narrowing results from, it is in first order a multiplicative modification to the dependence on the jump geometry in Eq. (4). Fig. 3 shows how static (short-range interactions) and dynamic effects (atomic jump vectors) lead to the experimentally accessible decay times and coherent line widths.

We confirmed above theory by measuring the decay times at 16 positions in the diffuse scattering regime, that is, away from Bragg reflections, see Fig. 3. All the data could be described by single exponential decays. The other necessary ingredient to Eq. (5), the short-range order intensity $I_{\text{SRO}}(\mathbf{q})$, was computed from the short-range order parameters up to the 13th neighbour shell as measured in Ref. 8 on the same sample and temperature range. Such measurements of short-range order parameters are an intricate task, as the detected diffuse intensity has to be corrected for contributions from, e.g., displacement scattering, thermal diffuse scattering and inelastic processes. Neglecting these contributions, a qualitative understanding could also be derived from the uncorrected intensities detected in the XPCS measurement, as our experimental data matched the published values of $I_{\text{SRO}}(\mathbf{q})$ within about 10%.

The experimental correlation times together with a fit according to Eq. (5) for nearest-neighbour exchanges are given in Fig. 4. For the fit of the 16 correlation times $\tau(\mathbf{q})$, just one parameter, the time between atomic exchanges $\tau_0$, is free. As all nearest-neighbour sites are equivalent, the exchange probabilities are equal to 1/12. The agreement between the measurements and the theory unambiguously proves that diffusion proceeds in this system via nearest-neighbour exchanges. This shows that XPCS has matured to the point where it reaches its full potential, i.e. to gauge the dynamics at atomic length scales.

The fitted mean Cu-Au exchange time $\tau_0$ at 543 K is $(2230 \pm 60)$ s. Via Eq. (5), dynamics on the atomic scale are completely specified by this value and the finding of nearest-neighbour jumps. All the information pertaining to the macroscopic scale, however, is given by the chemical diffusion coefficient, which is defined via the decay rate of concentration fluctuations in the macroscopic limit $\tilde{D} = \lim_{q \to 0} 1/(\tau(\mathbf{q})q^2)$. Conventionally it is measured through interdiffusion of two materials, in that case it is a function of macroscopic concentration; in our case, on the other hand, it is measured as the decay of equilibrium fluctuations at the constant concentration of 10%. We arrive at a value of $\tilde{D} = 2.62(7) \times 10^{-24}$ m²/s. This is by far the smallest bulk diffusivity ever measured while simultaneously achieving atomic spatial resolution.
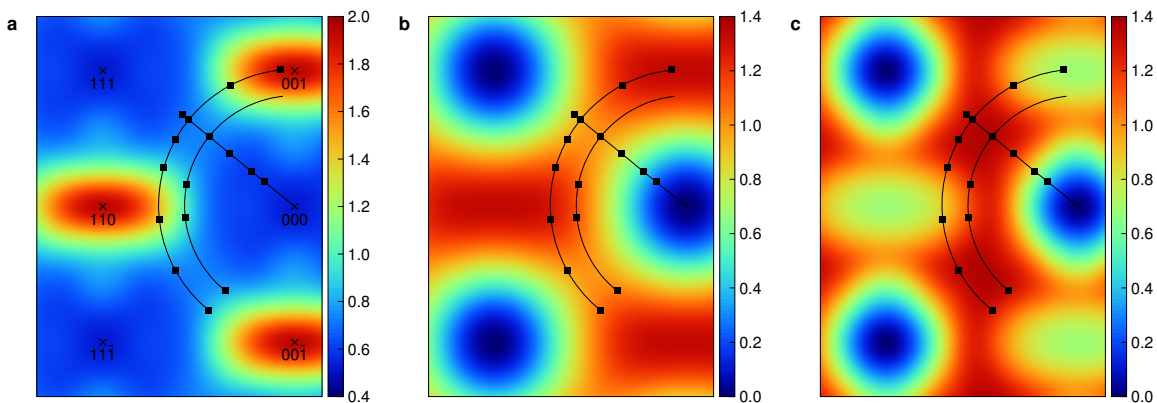
**Figure 3 | Visualisation of Eq. (5) for nearest-neighbour exchanges in the $(1\bar{1}0)$-plane in reciprocal space.** Values for the short-range order intensities are taken from Ref. 8. Black squares are positions of measurement projected onto the plane. The outer arc corresponds to Fig. 4 a), the inner arc to Fig. 4 b), the straight line to Fig. 4 c). a) The static scattered intensity $I_{SRO}(\mathbf{q})$, i.e. the numerator of Eq. (5). b) The incoherent linewidth $1 - \sum_i p_i \cos(\mathbf{s}_i \mathbf{q})$, i.e. the denominator of Eq. (5). c) The coherent linewidth $\left(1 - \sum_i p_i \cos(\mathbf{s}_i \mathbf{q})\right)/I_{SRO}$, i.e. the inverse of $\tau(\mathbf{q})$.
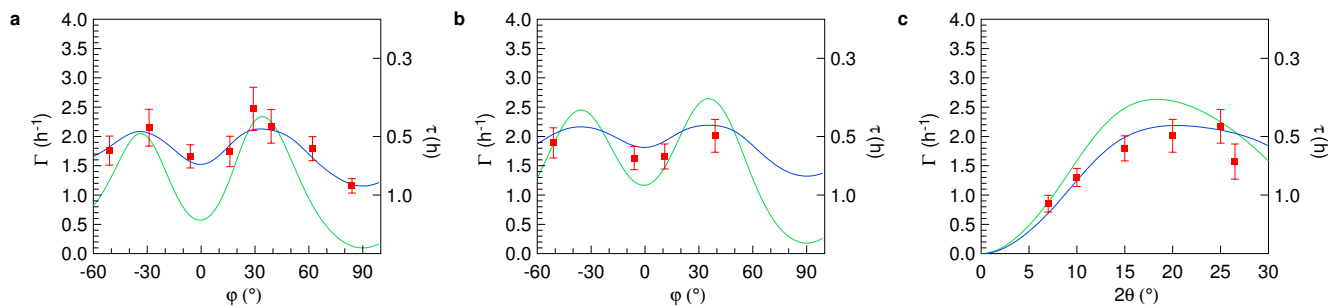


**Figure 4 | Experimental correlation times together with fits for three one-dimensional scans through reciprocal space.** Error bars are standard errors of the fitted correlation times. a) Azimuthal scan with fixed scattering angle $2\theta = 25°$, corresponding to $|\mathbf{q}| = 1.75\,\text{Å}^{-1}$. b) Azimuthal scan with fixed scattering angle $2\theta = 20°$, corresponding to $|\mathbf{q}| = 1.41\,\text{Å}^{-1}$. c) $2\theta$ scan with fixed azimuthal angle $\varphi = 39°$. For definition of angles see Fig. 3. Solid lines are one-parameter-fits according to Eq. (5), with only the factor $\tau_0$ free. A model with nearest-neighbour exchanges (blue line) reproduces our measurements well, whereas second-nearest-neighbour jumps (green line) cannot explain the data.

As stated above, the jump vectors $\mathbf{s}_i$ considered in Eq. (5) are the 12 nearest-neighbour vectors in the face-centred cubic lattice. It is known that diffusion via vacancies entails correlations between subsequent jumps of an atom. For the case of tracer diffusion, these effects have been treated quantitatively within the encounter model[17,18], giving effectively farther than nearest-neighbour jumps. The case of chemical diffusion, on the other hand, depends on a number of parameters such as concentration and interaction energies of the distinct species with themselves and the vacancy and has therefore to be treated for each distinct situation. Our results indicate that such effects are rather small in the present case, as there are no obvious systematic deviations in Fig. 4. Still, it has to be stressed that $\tau_0$ is not the literal mean time between exchanges, but rather the time between exchanges which are not undone within the next few steps of the vacancy.

Our results show that the dynamical behaviour of a given atom in a short-range ordered alloy—and every alloy is to some degree short-range ordered—depends on its neighbourhood. An atom of a given sort sitting on a given lattice site influences the occupancies in its surroundings in order to minimize the configurational energy. If now this atom leaves its site, this site will preferably become occupied by an atom of the same sort again, either the atom itself will hop back, or another one will take its place. This is because the diffusing vacancy has not completely disturbed the neighbourhood, a preference for the old occupation is still given. Clearly, with collective mechanisms, which are thought to dominate in glasses[19], where a number of neighbouring atoms move simultaneously, this is not the case. Such distinctions only coherent methods such as XPCS are sensitive to, as

they measure van Hove's pair correlation function. Conventional methods capable of resolving atomic dynamics (such as incoherent quasi-elastic neutron scattering, Mößbauer spectroscopy or nuclear resonant scattering), on the other hand, probe the self correlation function and average therefore over all the atoms irrespective of their neighbourhood.

In the present study, the sample is a binary alloy with moderate short-range order and the results can be described by a linear theory using the configurational energies (via the short-range order intensities) and the possible jump vectors. If one increased the degree of short-range order, in the present case either by lowering the temperature or increasing the Au content, the approximations would break down and higher terms would come into play. This is, however, not undesirable, since these higher terms contain additional information: already the first correction would depend on the transition frequencies between states, not only on the occupation probabilities. Thus, high-precision measurements of coherent correlation times would give access to hitherto experimentally elusive atomistic quantities such as saddle point energies of diffusing atoms as a function of the local configuration, constituting a much-needed touchstone for ab-initio calculations.

In conclusion, we have shown that it is possible to study dynamics with atomic resolution using coherent hard X-rays. As this method is a coherent method, it not only gives information on the dynamics of the "average" atom, but rather it shows the dynamics of an atom in the context of its neighbourhood. The presented results indicate that this information is far from trivial: even though there is no long-range order in the sample, different arrangements of the vicinity

of an atom lead to different dynamical behaviour. This is reflected in the variations of the decay times of fluctuations with position in reciprocal space and in this context de Gennes-narrowing in a substitutional alloy is observed for the first time. With the advent of future light sources with increased brilliance, both synchrotrons and X-ray free-electron lasers[20], we envision coherent X-ray scattering to become the method of choice for investigating the fundamental dynamics of matter, in our case the elementary atomic diffusion jump.

## Methods

The sample used was a single crystal of $Cu_{90}Au_{10}$, which initially was prepared for a diffuse X-ray scattering experiment[8]. Its composition was determined to be within 0.2 at.% of the nominal value by X-ray fluorescence analysis. The crystal was oriented by Laue backscattering, a slice with its surface parallel to the $(1\bar{1}0)$-plane was cut with a wire saw and ground to a thickness of 12 μm. The orientation was chosen in order to have access to all directions of high symmetry ($\langle 100 \rangle$, $\langle 110 \rangle$, and $\langle 111 \rangle$) without having to move the crystal.

The experiment was carried out at beamline ID10A at the European Synchrotron Radiation Facility in Grenoble, France. The X-ray beam was focused with a system of Be compound refractive lenses and deflected at a Si-(111) monochromator set to a photon energy of 8.0 keV (wavelength 1.55 Å), its energy resolution of $\frac{\Delta E}{E} = 1.4 \times 10^{-4}$ ensuring temporal coherence. Rollerblade slits were used to select a spatially partially coherent beam of 7 μm horizontal and 10 μm vertical size. The sample was mounted in a vacuum furnace in transmission geometry with the surface normal to the incident beam. The sample holder was resistively heated, the temperature was stable to 0.1 K, we estimate the actual temperature of the sample to agree with the nominal temperature within 3 K. Upstream, the furnace was equipped with a Kapton entrance window; downstream, the furnace was connected via flexible bellows to a flight tube filled with helium. After exiting the flight tube through a Kapton window, the scattered radiation was detected using a direct-illumination charge-coupled device (CCD) camera (Princeton Instruments, 1340 × 1300 pixels, 20 × 20 μm² pixel size). The sample-camera distance of 1.32 m was optimized for gaining maximum scattering intensity without sacrificing contrast. Thanks to this setup, when changing the scattering vector, only the detector and the flight tube were moved, the sample stayed fixed during the whole experiment. After the experiment the sample was left in the holder and the exact orientation was measured.

Time series of the scattered intensity of typically 2 hours duration were taken with 10 s exposure per frame. As proposed by Livet et al.[21], these frames were processed to time vectors of the number of detected photons in each pixel. The count rates were typically 3 photons per hour and pixel. Since the scattering vector **q** varies over the detector only by about 4%, all the pixels were treated as equivalent within the experimental accuracy. The auto-correlation functions of the respective measurement runs were each fitted with separate coherence factors $\beta$ and correlation times $\tau$. The values of $\beta$ were in the range of 3%.

The stability of the setup was checked by analysing the scattered intensity of a static sample at room temperature. Over a time of 2 hours, only a very insignificant decay of correlation leading to an apparent correlation time of days was detected, therefore the setup was judged as stable. Still, sometimes during measurements abrupt decays of correlation were detected (by fitting the one-time autocorrelation function obtained from subsets of the data or by inspecting the two-time autocorrelation function). These were excluded from the evaluation. The fitted $\beta$ of the control experiment agreed with the values of $\beta$ of the measurement runs, indicating that no fast component was missed.

## References

1. Vogl, G. & Sepiol, B. The Elementary Diffusion Step in Metals Studied by the Interference of Gamma-Rays, X-Rays and Neutrons. In Heitjans, P. & Kärger, J. (eds.) *Diffusion in Condensed Matter*, 65–92 (Springer, Berlin/Heidelberg, 2005).
2. Sutton, M. *et al.* Observation of speckle by diffraction with coherent X-rays. *Nature (London)* **352**, 608–610 (1991).
3. Brauer, S. *et al.* X-ray intensity fluctuation spectroscopy observation of critical dynamics in Fe₃Al. *Phys. Rev. Lett.* **74**, 2010–2013 (1995).
4. Dierker, S., Pindak, R., Fleming, R., Robinson, I. & Berman, L. X-ray photon correlation spectroscopy study of Brownian motion of gold colloids in glycerol. *Phys. Rev. Lett.* **75**, 449–452 (1995).
5. Shpyrko, O. G. *et al.* Direct measurement of antiferromagnetic domain fluctuations. *Nature (London)* **447**, 68–71 (2007).
6. Mehrer, H. *Diffusion in Solids: Fundamentals, Methods, Materials, Diffusion-Controlled Processes* (Springer, Berlin/Heidelberg, 2007).
7. Springer, T. & Lechner, R. E. Diffusion studies of solids by quasielastic neutron scattering. In Heitjans, P. & Kärger, J. (eds.) *Diffusion in Condensed Matter*, 93–164 (Springer, Berlin/Heidelberg, 2005).
8. Schönfeld, B., Portmann, M. J., Yu, S. Y. & Kostorz, G. The type of order in Cu − 10 at.% Au – evidence from the diffuse scattering of X-rays. *Acta mater.* **47**, 1413–1416 (1999).
9. van Hove, L. Correlations in space and time and Born approximation scattering in systems of interacting particles. *Phys. Rev.* **95**, 249–262 (1954).
10. Sutton, M. X-ray intensity fluctuation spectroscopy. In Hippert, F., Geissler, E., Hodeau, J., Lelièvre-Berna, E. & Regnard, J. (eds.) *Neutron and X-ray Spectroscopy*, 297–318 (Springer Netherlands, 2006).
11. Chudley, C. T. & Elliott, R. J. Neutron scattering from a liquid on a jump diffusion model. *Proc. Phys. Soc.* **77**, 353–361 (1961).
12. Fujikawa, S., Werner, M., Mehrer, H. & Seeger, A. Diffusion of Gold in Copper Over a Wide Range of Temperature. In *Mater. Sci. Forum*, vol. 15, 431–436 (1986).
13. de Gennes, P. G. Liquid dynamics and inelastic scattering of neutrons. *Physica* **25**, 825–839 (1959).
14. Dasannacharya, B. A. & Rao, K. R. Neutron scattering from liquid argon. *Phys. Rev.* **137**, A417–427 (1965).
15. Caronna, C., Chushkin, Y., Madsen, A. & Cupane, A. Dynamics of nanoparticles in a supercooled liquid. *Phys. Rev. Lett.* **100**, 055702 (2008).
16. Sinha, S. K. & Ross, D. K. Self-consistent density response function method for dynamics of light interstitials in crystals. *Physica B* **149**, 51–56 (1988).
17. Wolf, D. Theory of Mössbauer line broadening due to correlated diffusion in crystals. *Appl. Phys. Lett.* **30**, 617–619 (1977).
18. Sholl, C. A. Diffusion correlation factors and atomic displacements for the vacancy mechanism. *J. Phys. C* **14**, 2723–2729 (1981).
19. Teichler, H. Structural dynamics on the μs scale in molecular-dynamics simulated, deeply undercooled, glass-forming Ni₀.₅Zr₀.₅. *J. Non-Cryst. Solids* **293-295**, 339–344 (2001).
20. Grübel, G., Stephenson, G., Gutt, C., Sinn, H. & Tschentscher, T. XPCS at the European X-ray free electron laser facility. *Nucl. Instrum. Meth. B* **262**, 357–367 (2007).
21. Livet, F. *et al.* Using direct illumination ccds as high-resolution area detectors for X-ray scattering. *Nucl. Instrum. Meth. A* **451**, 596–609 (2000).

## Author contributions

G.V. and B.S. conceived the idea of the experiment, M.L. realised it. B.S. constructed the experimental apparatus. All authors were present at the experiment. M.L. analysed the data and wrote the paper. All authors discussed the results and implications and provided input to the manuscript at all stages.